Detection of "Cold" Spectra from a Room-Temperature Ensemble: Magnetic Rotation Spectroscopy with Simple Interpretation in Terms of Molecular Pendular States

Alkwin Slenczka[†]

Institut für Physikalische und Theoretische Chemie, Universität Regensburg, D-93040 Regensburg, Federal Republic of Germany

Received: April 14, 1997; In Final Form: July 21, 1997[⊗]

The anisotropic orientation of the figure axis of pendular molecules is directly detected by polarization spectroscopy for ICl in the excited A $^3\Pi_1$ state. A simple geometric model is outlined that simulates all spectral features over a wide range of experimental parameters, without any fitting procedure. The experimental technique, closely related to magnetic rotation spectroscopy, strongly favors low rotational states and is also selective for ΔJ within a rotational band. Spectra obtained using a gas cell at room temperature thereby become even sparser and simpler than can be attained by cooling molecules to a few kelvin. Moreover, it provides a technique for local measurement of electric or magnetic field strengths without mechanical devices.

1. Introduction

The experimental and theoretical study of molecular pendular states[1−3] and the implementation of pendular states in stereodynamic scattering experiments[4] has become an interesting field in molecular physics. Most experiments thus far deal with molecules having a body-fixed permanent electric or magnetic dipole moment. Recently, however, it has been demonstrated theoretically[5] and experimentally[6] that pendularization also works for induced dipole moments. For pendular states the free rotation of a dipolar molecule changes into a small-angle libration if the molecule is put into a strong homogeneous electric or magnetic field. The dipole moment and thus the molecular axis are aligned or even oriented in the laboratory frame. Direct experimental evidence for this effect has been extracted from fluorescence excitation spectra of pendular states that differ substantially from free rotor spectra. Since transition dipole moments are polarized within the body-fixed frame of the molecule, it should be easy to implement a spectroscopic technique to look at the alignment of pendular molecules. However, up to now no experiment has been performed measuring directly the anisotropy of the molecular orientation.

This consideration leads to the application of polarization spectroscopy to pendular states. It is based on an optical anisotropy that used to be created by a pump laser in an absorbing sample.[7] In our case the anisotropy is induced by a dc homogeneous field that acts on the free rotation of a dipolar molecule. The polarization of incident linearly polarized light is changed by an anisotropic absorption of the sample. The plane of polarization of the transmitted light is rotated by an angle depending on the optical anisotropy of the medium. Depending on the transition moment and orientation of the field direction with respect to the laser beam axis, the polarization can also be changed into elliptically polarized light. The high sensitivity of this technique is based on the suppression of noise and background terms in the signal by orders of magnitude.[7] A prototypical study demonstrating the sensitivity of this technique is the polarized hole-burning spectroscopy of matrix-isolated molecules with polarized light. By application of polarization spectroscopy, the background subtraction procedure, which usually increases noise, is changed into a null background, and the detection scheme provides high signal to noise.[8]

The idea of measuring the alignment of molecules in the laboratory frame is related to the technique of magnetic rotation (MR) spectroscopy.[9] In MR experiments the clockwise and counterclockwise polarization of $\Delta M_J = \pm 1$ transition dipole moments of Zeeman sublevels created by a magnetic field coaxial to the laser beam axis causes an optical anisotropy. This is the Faraday effect. In contrast to the Faraday effect, the magnetic field in our experiment is perpendicular to the laser beam axis. In magnetooptic spectroscopy (MOS) this experimental geometry is known as the Voigt effect. Faraday and Voigt effects are essentially the same physical process described as forward scattering magnetooptical spectroscopy.[10] The change in geometry enables study of the anisotropy of transition dipole moments polarized in the plane perpendicular to the laser beam axis with linearly polarized laser light. For pendular molecules the anisotropy of the transition dipole moment is equivalent to the anisotropy of the molecular axis.

A characteristic feature of MOS spectroscopy is high selectivity for low rotational states of paramagnetic molecules. The selectivity is so strong that low field MOS spectra can easily compete with other techniques such as cooling by supersonic expansion. Besides its low J selectivity, MOS spectroscopy was found to be selective for a specific $\Delta J = \Delta\Omega$ branch within a rotational band.[9] Therefore, it is easy to determine a band origin and the rotational constant for the lower and upper electronic states involved in the transition. This is not always easy for overlapping branches of fluorescence spectra taken, for example, in a molecular beam apparatus. All these features appear in the polarization spectra of pendular states obtained with our experimental geometry. In addition to detection of molecular alignment, the technique offers a dramatic simplification of molecular spectra, especially at very low field strengths.

Here we report an experiment making use of the paramagnetism of the A state of ICl. The results demonstrate the power of polarization spectroscopy applied to pendular states, without any other signal-enhancing technique. In interpretation of the spectra, we employ a simple approximate model for pendular states. This provides insight into the physical origin of the optical anisotropy and treats all features of the spectra, including line positions, line structures, intensities, and selectivities. Without any adjustable parameters, the treatment accounts quantitatively for all our experimental spectra taken over a range of 2 orders of magnitude in magnetic field strength.

[†] e-mail: alkwin.slenczka@chemie.uni-regensburg.de.

[⊗] Abstract published in *Advance ACS Abstracts,* September 15, 1997.

S1089-5639(97)01269-3 CCC: $14.00

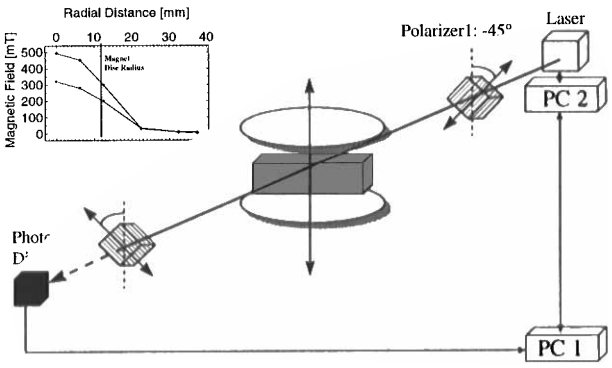

Figure 1. Experimental setup of the polarization spectroscopic experiment on pendular molecules (see text). Inset shows magnetic field strength as function of radial distance for two different numbers of magnet discs in the pile (see text).

Following a brief description in section 2 of the experimental setup, we present in section 3 the polarization spectra for pendular states of ICl. The theoretical analysis is given in section 4, including discussion of simple approximations and calculation of spectra. Finally, in section 5 we outline an extension of this spectroscopic technique, which is applicable even to nonpolar or nonmagnetic molecules in the gas phase, by creating optical anisotropy by interaction of a nonresonant laser field with the molecular polarizability.[5]

2. Experimental Setup

Figure 1 shows the setup of the absorption experiment. It consists of the usual components required for MR spectroscopy, namely, a frequency tunable light source, two polarizers, a sample cell, and a light detector. The light source is a computer-controlled Ar^+ ion laser pumped single-mode ring dye laser (Coherent 899-29) with Rh6G dye. The first polarizer ensures that the output of the laser is linearly polarized with polarization plane at $-45°$ with respect to the magnetic field vector. With the second polarizer 90° rotated with respect to the first one the extinction ratio is $\Xi < 10^{-6}$. The windows of the evacuated sample cell between the polarizers reduce the extinction to $\Xi = 10^{-6}$; this is mostly due to strain-induced birefringence.

In contrast to typical MRS experiments, the magnetic field is perpendicular to the laser beam direction. The field is generated by a small U-shaped permanent magnet, comprised of a pile of disc-shaped permanent magnets and ferromagnetic metal plates. The field strength in the center of the 14 mm gap can reach up to 0.5 T, depending on the number of magnets in the pile. The radial field strength distribution was measured with a Hall probe and is shown in the inset of Figure 1 for two sets of magnets in the pile. The sample cell is a cubic cell made of silica plates of optical quality. The laser path length through the cell is 1 cm. In preparing the sample, the cell was cleaned, evacuated and refilled with 1 atm of Ar, adding solid ICl, and finally evacuated again. The pressure of ICl in the cell is its vapor pressure at room temperature. The detector is a photodiode with a voltage amplifier. The signal is digitized by an analog-to-digital converter (not shown in Figure 1) and fed into a computer (PC1). In addition, this computer controls the dye laser computer (PC2) and synchronizes frequency steps and data sampling. No additional noise reducing techniques such as lock-in or FM spectroscopy is used.

3. Experimental Results

Figure 2 shows two absorption spectra taken without the magnetic field. The upper trace shows the absorption without the second polarizer, taken with an attenuated laser power of

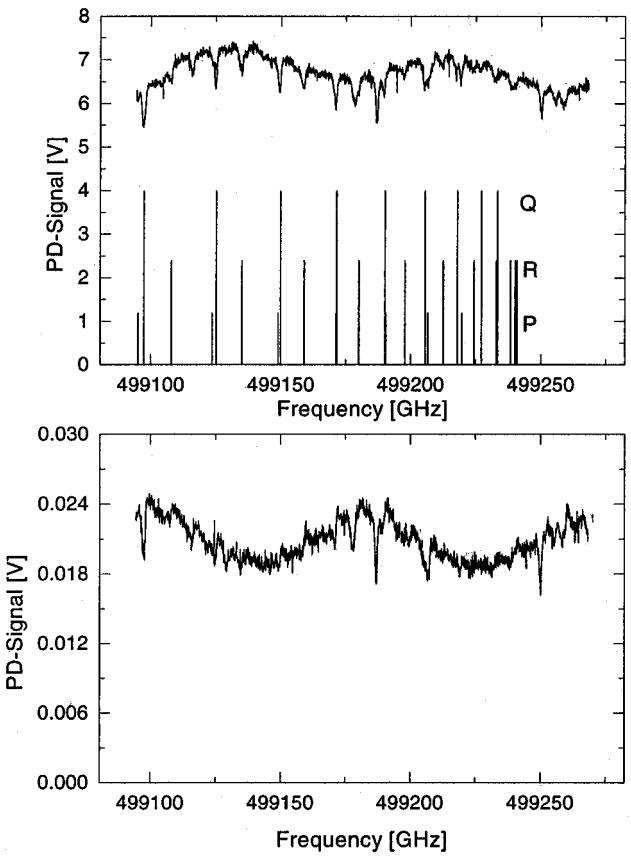

Figure 2. Absorption spectra of ICl in the regime of the A(19)−X(0) band head. Upper spectrum: laser power 38 mW; lines represent calculated P, Q, and R branches of the band; hyperfine structure is omitted. Lower spectrum: laser power 300 mW; residual transmission detected behind the second polarizer rotated by 90° with respect to the first; PD signal is amplified by a factor of 100 compared to upper spectrum.

38 mW to prevent saturation of the detector. The lower trace shows the same spectrum taken with an exactly 90° rotated second polarizer with respect to the first. The input power of the laser is 300 mW, and the amplification of the photodiode signal is increased by a factor of 10^2. Both spectra demonstrate the sensitivity and resolution of simple absorption spectroscopy at room temperature. The scan range covers the ICl(A(19)−X(0)) band head, obscured by a variety of rotational lines from other vibrational bands or I_2 impurity. It is impossible to determine the head or origin of the band. The stick spectrum in the upper part of Figure 2 shows the calculated line positions of the P, R, and Q branches. The hyperfine structure of ICl is omitted in this calculation. The undulatory structure in the base line arises from interference effects caused by the sample cell windows.

In contrast, the upper trace in Figure 3 is taken with the pair of polarizers rotated exactly 90° with respect to each other and the sample between the polarizers within the gap of the permanent magnet. The magnetic field vector points at $\pm 45°$ with respect to both polarizers. The field strength H is 320 mT. The input laser power, amplification factor of the photodiode signal, and scaling of the signal axis are identical with the lower spectrum of Figure 2. The spectral features appear at the same frequency position as the calculated line positions of the field-free ICl(A(19)−X(0)) rotational band transitions, except for the lowest rotational states in the band head. The signal-to-noise ratio is orders of magnitude larger than for the absorption spectra (Figure 2). All features blue-shifted relative to the red-degraded band head and also some spectral features of the absorption spectrum within the range of the band head

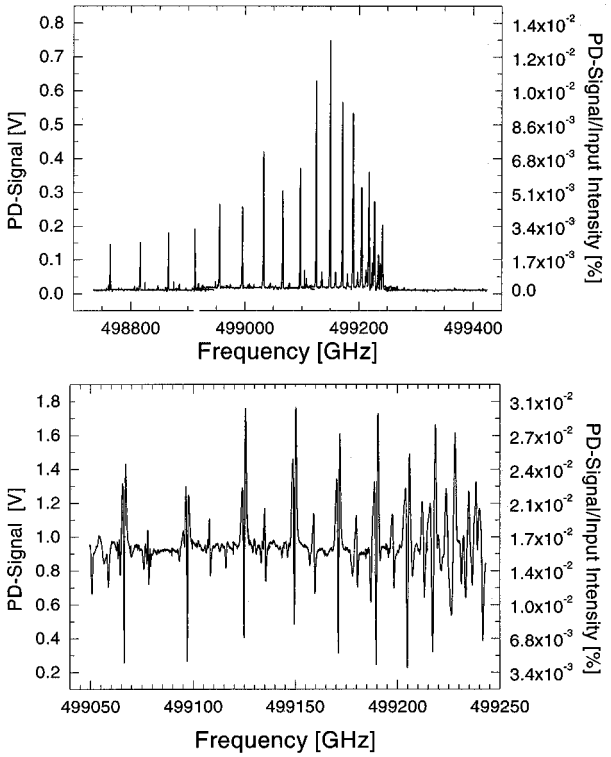

Figure 3. Polarization spectra of the ICl(A(19)−X(0)) pendulum band head. Upper spectrum: with exactly 90° crossed polarizers; magnetic field 320 mT. Lower spectrum: second polarizer detuned by $+\zeta$ from exactly 90° crossed position; negative lines have sign (ξ) equal to sign(ζ) and positive lines have $-$sign(ξ) equal to sign(ζ); magnetic field strength is 400 mT.

(Figure 2) do not appear in the spectrum. The Q branch dominates in intensity while the P and R branches nearly disappear in the spectrum, except for the lowest rotational states within the head of the band. The intensity distribution within the Q branch shows a maximum for $J = 7$. This is in contrast to the maximum at $J = 30$ expected for a fluorescence excitation spectrum of ICl recorded at room temperature. A maximum at $J = 7$ would appear at a temperature of only 20 K.

The signal is due to rotation of the plane of polarization of the transmitted laser light. Our interpretation is based on differential absorption of light polarized parallel or perpendicular with respect to the magnetic field. We do not include the phase in our model calculations. This effect is well-known from Zeeman spectra for $\Delta M = \pm 1$ and $\Delta M = 0$ transitions. Since the linearly polarized input laser field E_0 (as shown in the upper part of Figure 4) is a coherent superposition of two plane waves $E_\perp$ and $E_\parallel$ polarized parallel and perpendicular to H, equal in amplitude, an anisotropic absorption results in different amplitudes of both field components and thus in a rotation of the plane of polarization of the coherent superposition. In the same way the polarization of the transmitted light can be split into a coherent superposition of two plane waves polarized parallel and perpendicular to the second polarizer. The parallel component E_T passes the second polarizer and is detected by the photodiode. This is illustrated in the upper part of Figure 4. The sensitivity of the experimental technique critically depends on the extinction ratio Ξ of the polarizers.

A slight deviation from the exact 90° rotation of the second polarizer with respect to the first one allows the direction of rotation of the polarization plane to be determined. Already the incoming wave has a component E_{T_0} parallel to the second polarizer. The spectrum shows a base line signal level. Rotation of the polarization in the direction of the detuning angle

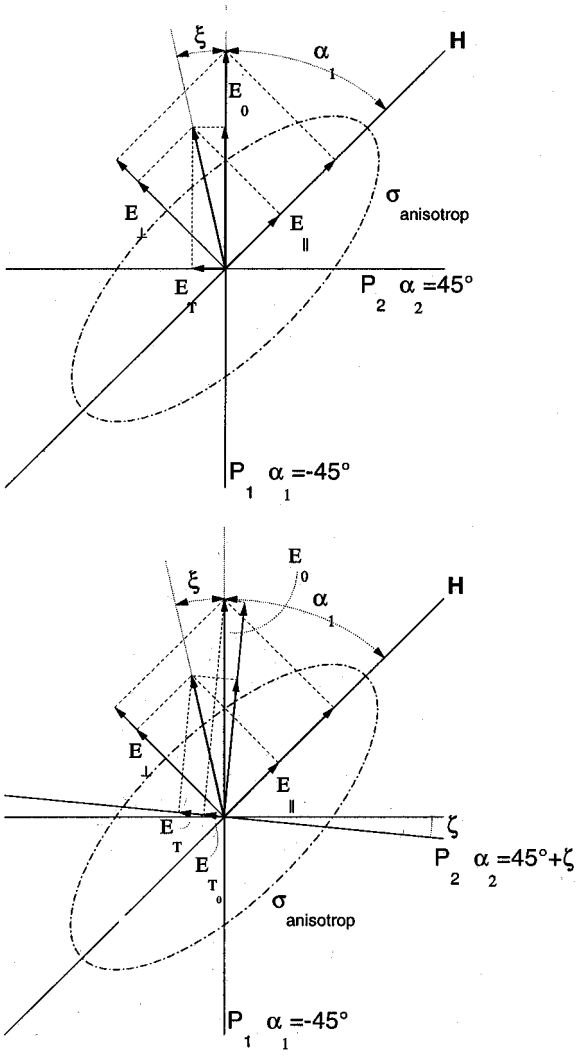

Figure 4. Vector diagram for magnetic rotation spectroscopy. Incoming electromagnetic wave polarization denoted by E_0; transmitted wave polarization by E_T; angle of rotation of the plane of polarization of the incoming wave by ξ. Upper part with diagram pertains to polarizers P_1 and P_2 rotated by exactly 90° with respect to each other. Lower diagram has the second polarizer P_2 detuned by $+\zeta$, and the base line transmitted wave is E_{T_0}. Both diagrams show an anisotropic absorption coefficient $\sigma_{anisotrop}$ (dash-dotted ellipse).

ζ of the second polarizer occurs as a negative signal, and vice versa. This is exhibited in the lower part of Figure 4, including the anisotropy of the absorption coefficient $\sigma_{anisotrop}$ of the sample (dash-dotted ellipse). The experimental observation is shown in the lower part of Figure 3. The magnetic field strength is 400 mT, and the detuning angle ζ of the second polarizer is about $+1°$. For nonoverlapping transitions the line shape changes from a single positive peak into either a negative line center and positive shoulders, or vice versa. The first line shape represents the Q branch and the latter the P and R branch. The background signal level increases by orders of magnitude compared to the upper spectrum in Figure 3. The detuning angle was chosen in order to reach a background level of at least the peak intensity of the signals seen in the spectrum with the polarizers rotated by exactly 90° with respect to each other. Otherwise, it may happen that the rotation angle ξ of the polarization plane in the direction of the detuning of the second polarizer becomes larger than the detuning angle ζ. This would cause additional features in the spectra. Both spectra in Figure 3 show two ordinates, one giving the PD voltage and the other giving the transmitted intensity normalized to the input intensity.

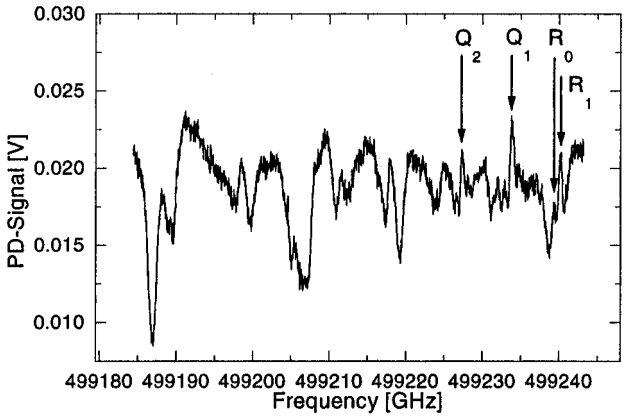

Figure 5. Polarization spectrum of ICl pendulum with polarizers rotated by exactly 90° with respect to each other; magnetic field strength about 8 mT; polarization lines are marked by arrows.

The low J state selectivity is again demonstrated experimentally in Figure 5. The magnetic field strength is only a few millitesla, and the polarizers were rotated by 90° with respect to each other. At this low field strength even the lowest rotational states show only small Zeeman splitting centered around the free rotor J level. The Q_2, Q_1, R_1, and the R_0 lines appear as small but sharp positive peaks. All other features disappear in the residual simple absorption spectrum of the room-temperature ICl sample. In the rigid rotor approximation the distance between Q_1 and R_0 is twice the rotational constant B'' of the lower state, and that between Q_1 and R_1 is 4 times the rotational constant B' of the upper state. A very rough reading of the peak distances from Figure 5 leads to values that are 10% smaller than those given in ref 17. A better result will be obtained (i) by including the peak maximum shift due to the nonhorizontal background level and (ii) by careful study of the peak shape of the lines that depends on the total spectral resolution of the experimental setup. The low J selectivity at low field strength generally found for MOS is unique. To thermally select these few lines would require a temperature of about 0.5 K. It is much harder (if not impossible) to select these lines from molecular jet spectra at a rotational temperature of a few kelvin.[19]

Polarization spectra of pendular states of molecules with a body-fixed electric dipole moment created in a static electric field have also been measured and will be the subject of a forthcoming paper. As with Zeeman splitting or pendular fluorescence spectra,[20] magnetooptic spectra can be used to determine magnetic field strengths. The polarization spectra of electric pendular states can also be used to measure electric field strengths with high local resolution. This aspect of our experiment is a byproduct, and it represents one among many different methods used for optical measurements of electric or magnetic field strengths with local and temporal resolution. Field measurements in closed environments like plasmas are of particular interest for optical methods. Compared to laser-induced fluorescence (LIF) spectroscopy,[21] polarization spectroscopy is advantageous in signal-to-noise level as outlined in ref 9.

4. Calculation of the Spectra

First, we give a short summary of the theory of pendular states as far as it is necessary for calculating eigenstates, eigenenergies, and line strength factors. Then we present a procedure to simulate polarization spectra of pendular states, discussing in detail the approximations we use for the final really simple equation.

Exact eigenenergies and eigenstates of a rotating magnetic dipole in a homogeneous magnetic field need to be calculated. This is done by solving the Schrödinger equation for the system with the Hamiltonian[1]

$$H_r = B[\mathbf{J}^2 - \Omega^2 - \omega \cos(\theta)] \tag{1}$$

with B the rotational constant, Ω the projection of the electronic angular momentum on the molecular figure axis, and $\omega = \mu H/B$ the dimensionless interaction parameter that gives the potential energy of the dipole μ in the magnetic field H. The eigenstates are expanded in terms of the field-free wave functions:

$$|\tilde{J},\Omega,M;\omega\rangle = \sum_J a_{J,\Omega,M}(\omega)|J,\Omega,M\rangle \tag{2}$$

where the summation runs over J, which is not a good quantum number for the pendular states. The $a_{J,\Omega,M}(\omega)$ are expansion coefficients of the respective free rotor function. The number of J states involved significantly in the summation increases with increasing magnetic field strength as does the alignment of the molecular axis. This is an expression of the uncertainty principle between the conjugate quantities angle and angular momentum. $\tilde{J}$ is the rotational quantum number of the field-free state to which the pendular state converges adiabatically with decreasing field strength. The quantum mechanical pendulum was treated early in the development quantum mechanics.[11] In his 1928 paper, *The Physical Pendulum in Quantum Mechanics*, E. U. Condon stated that "*it can't be without interest...*[since it]*...played such a great role in the study of analytic mechanics*". His foresight proved to be justified, and since then Condon's treatment of a planar quantum mechanical pendulum has been extended to a spherical pendulum by several authors,[1,12−16] culminating in a very detailed discussion of this problem including the spectroscopy of pendular states in ref 3.

Since the ICl electronic ground state X is not affected by the magnetic field (it has no magnetic dipole moment and is a Σ state with $\Omega'' = 0$), we have to calculate the line-strength factors for the ground state as a free rotor and the excited A state as a symmetric top pendular state given by

$$S(\tilde{J}\leftarrow J'') = \left|\sum_{J,q} a_{J',\Omega',M'}(\omega)(2J''+1)^{1/2}(2J'+1)^{1/2} \times \begin{pmatrix} J'' & 1 & J' \\ -M'' & Q & M' \end{pmatrix}\begin{pmatrix} J'' & 1 & J' \\ 0 & q & \Omega' \end{pmatrix}\right|^2 \tag{3}$$

Here $Q = 0, \pm 1$ designates the spherical components in the laboratory frame of the electric field vector of the laser, while $q = 0, \pm 1$ designates those in the molecular body-fixed frame of the transition dipole operator of the molecule. These factors determine the ΔM and $\Delta\Omega$ transitions, respectively. The $\Pi-\Sigma$ transitions between the A and X state of ICl have a nonzero component of the transition dipole moment only for $q = \pm 1$. The summation runs over all J' involved in the pendular state given in eq 2 and over $q = \pm 1$ transitions. In addition to the change in the eigenenergies of pendular states, the strict $\Delta\tilde{J}$ selection rule is lifted. As the terms in eq 2 with $J = \tilde{J} \pm n$ (n a positive integer) start to grow, there appear additional transitions with $\Delta\tilde{J} = \pm(n+1)$.

The transmission of the laser field component parallel or perpendicular to the magnetic field is determined by

$$E_{\perp,\parallel}/E_0 = \exp(-\sigma_{\perp,\parallel} nl) \tag{4}$$

The exponent includes the particle density n, the path length l of the laser through the sample cell, and the absorption cross

section $\sigma_{||}$ or $\sigma_{\perp}$. It is a function of the line strength factor S, the respective Boltzmann factor for the $|J'',M''\rangle$ state, and finally a line shape factor. The $\sigma_{\perp}$ includes the S factor for $\Delta M = \pm 1$ and $\sigma_{||}$ that for $\Delta M = 0$. The transitions are polarized perpendicular and parallel to the molecular axis. The axis of a molecular pendulum becomes aligned parallel to the field direction. In our experiment the line shape is determined by the Doppler width of ICl at room temperature.

To determine the angle ξ of rotation of the plane of polarization, we calculate the ratio $E_{\perp}/E_{||}$. The upper diagram of Figure 4 shows $E_{\perp}$ and $E_{||}$, and the arctan of their ratio is the angle $45° - \xi$. The electromagnetic field behind the second polarizer is given by the projection of the transmitted field onto the axis of the second polarizer

$$E_T = [(E_{\perp}/E_0)^2 + (E_{||}/E_0)^2]^{1/2} \sin \xi \qquad (5)$$

This is also displayed in the vector diagram of Figure 4. The calculation proceeds in exactly the same way for the absorbed part of the electromagnetic wave. The arctan of the ratio of $1 - (E_{\perp}/E_0)$ and $1 - (E_{||}/E_0)$ determines an angle $45° - \beta$. Equation 4 can be rewritten as

$$E_T = [(1 - E_{\perp}/E_0)^2 + (1 - E_{||}/E_0)^2]^{1/2} \sin \beta \qquad (6)$$

Taylor series expansion of eq 4 up to the second term reduces the ratio $1 - (E_{||}/E_0)/1 - (E_{\perp}/E_0)$ to the ratio of the line strength factors including line shape times Boltzmann factors $\rho_B(J'',M'')S(\nu,\Delta M{=}0)/\rho_B(J'',M'')S(\nu,\Delta M{=}\pm 1)$. Here we designate by $S(\nu,\Delta M{=}0,\pm 1)$ the Doppler broadened line shape weighted with the line strength factor S of eq 3. All other quantities in the absorption coefficient cancel out. The same holds for the squared terms in the square root factor of eq 6, so that the transmitted relative intensity is given by the square of

$$E_T \propto [(S(\nu,\Delta M{=}\pm 1))^2 + (S(\nu,\Delta M{=}0))^2]^{1/2} \sin(45° - \delta) \qquad (7)$$

where $\delta \equiv \arctan\{S(\nu,\Delta M{=}0)/S(\nu,\Delta M{=}\pm 1)\}$. The Boltzmann factor for the rotational levels has been omitted in eq 7. For the calculation of spectra with slightly detuned polarizers, eq 7 is replaced by

$$E_T \propto [(S(\nu,\Delta M{=}\pm 1))^2 + (S(\nu,\Delta M{=}0))^2]^{1/2} \sin\{45° \pm \zeta - \delta\} + E_0 \sin(\pm\zeta) \qquad (8)$$

with ζ the detuning angle of the polarizer (see lower part of Figure 4). The last term in eq 8 is the base line transmission E_{To}. For $\zeta = 0$ eq 8 is identical with eq 7. This equation is a substantial simplification of the exact theory outlined in refs 9 and 10 for magnetic rotation spectroscopy. Guided by the simple picture of pendular molecules aligned parallel to the magnetic field, eq 8 is nothing but the resultant anisotropy of the absorption without phase information. We have found it quite adequate to simulate the polarization spectra of pendular states of ICl. Spectroscopic constants for ICl are taken from ref 17. Hyperfine structure does not influence the pendular spectra at the experimental resolution[18] and is omitted. The interaction parameter ω' is calculated from the measured magnetic field strengths and the known magnetic dipole moment of the A state of ICl. The calculations do not involve any fitted parameters.

The upper part of Figure 6 shows a spectrum calculated for the experimental parameters corresponding to the upper part of Figure 3. For the ground state $\omega'' = 0$ and for the A state $\omega' = 2.43$, which corresponds to a field strength of 320 mT. The

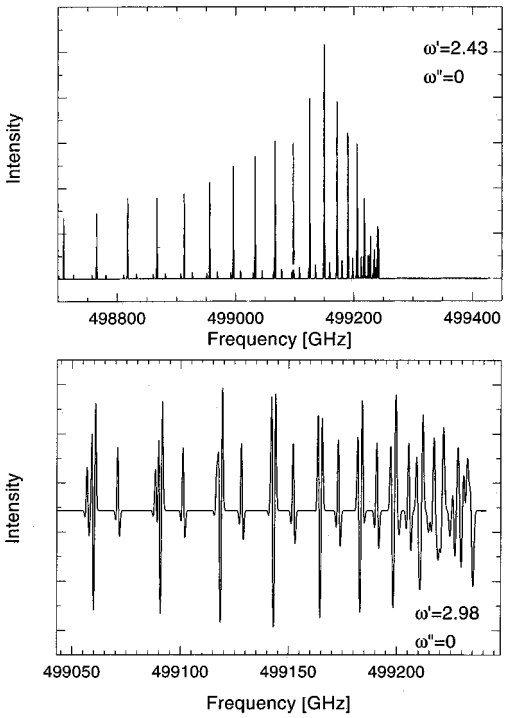

Figure 6. Simulated polarization spectra for ICl pendular states. Upper spectrum: $\omega' = 2.43$; polarizers rotated by exactly 90° with respect to each other. Lower part: $\omega' = 2.98$; detuning angle $\zeta = 1°$. Both spectra simulate the experimental results presented in Figure 3.

computed Q branch appears with high intensities and has its maximum for Q_7, as in the experimental spectrum. Also, the computed P and R branches have low intensities and disappear in the red half of the spectrum. The higher J state transitions match exactly the free rotor transitions of ICl while the structure in the band head differs significantly. At the chosen magnetic field strength, high J' states are still in the Zeeman regime and show symmetric and small $M_{J'}$ level splittings centered around the field-free $\tilde{J}$ level. For the low J' levels the rotational energy is less than the potential energy of the dipole in the field. The molecule thus becomes a real pendulum, and its eigenenergy differs significantly from the free rotor level (also for $M_{J'} = 0$) and so do the transition energies. This explains the deviation of the band head line structure from the free rotor spectrum.

The lower part of Figure 6 shows the calculated spectrum for interaction parameters of $\omega'' = 0$ and $\omega' = 2.98$. These are the values for a magnetic field strength of 400 mT. The detuning angle in eq 8 is $\zeta = 1°$, and the parameters coincide with the experimental conditions of the lower spectrum of Figure 3. All characteristic features in the band head are reproduced. In addition, until the red end of the spectrum, all features of every transition are reproduced. The lines of the Q branch show a negative peak center and positive shoulders, which is opposite to the P and R branches. The multiple up−down structure of the first and the third peak at the red end is an overlap of a P and Q branch line. Only the peak levels in the simulated spectra do not agree perfectly with the experiment. This can be attributed to two experimental limitations: (i) The magnetic field strength has a radial distribution as shown in Figure 1 (inset). The interaction parameter ω' was determined from the maximum center value of the magnetic field strength, but the laser path through the sample cell covers a 10 mm path centered in the gap of the magnet parallel to the radius of the magnet discs. (ii) The calculations assume a magnetic field vector rotated by exactly 45° to the plane of polarization of the input light. Even a deviation of about 0.1° could alter the positive and negative signal levels of the spectra substantially.

The line shape of the spectra with detuned polarizers (lower trace in Figure 6) is due to the A state paramagnetism. At the experimental field strength the eigenenergies of the $M_{J'}$ levels of the A state increase with decreasing M_J' value. Those of the X state remain degenerate. In the P, Q, and R branches, the $\Delta M = +1$ and -1 components are blue- and red-shifted, respectively, by about one M_J' level splitting with respect to $\Delta M = 0$. For $\Delta M = 0$, the line strength factors (eq 3) of the Q branch maximize at high $|M_J|$ values, but they maximize at $M_J = 0$ for $\Delta M = \pm 1$. The P and R branches show the opposite behavior. This explains the relative polarizations of line center and shoulders in the spectra. If both the upper and lower electronic state were paramagnetic, the line shape would look much more complicated depending on the M_J splittings in both states. As for the free rotor ΔJ branches, there appear ΔM branches with an origin and a head in one of the $\Delta M = \pm 1$ branches.

The line intensities in particular as functions of magnetic field strength or the interaction parameter ω' reflect the evolution of the expansion coefficients in eq 2. For the special case of the $\Pi-\Sigma$ transition of ICl only the expansion coefficients $a_{J',\Omega',M'}(\omega')$ with $J' = J''$ and $J'' \pm 1$ contribute to the line strength factor of the pendular P, Q, and R branches. Their dependence on ω' can be determined from the intensities. This requires a deconvolution of the lines with a function including the $M_{J'}$ level splitting and the experimental resolution. In the same way the other expansion coefficients can be extracted from the $\Delta\tilde{J} = \pm n$ ($n > 1$) transition intensities. The $M_{J'}$ level splitting, which is directly related to the alignment of the molecule, determines the optical anisotropy and thus also the line intensities. This is the major reason for the intensity distribution within a band. The low intensities of the P and R branches are due to the smaller values of the Clebsch−Gordan coefficients in eq 3 compared to the Q branch. This result is in contrast to the finding for the Faraday effect geometry in ref 9. This experiment using NiH shows a ΔJ branch selection for $\Delta J = \Delta\Omega$ which was found for two electronic transitions: one with $\Delta\Omega = 0$ selecting the Q branch the other with $\Delta\Omega = 1$ selecting the R branch. For both investigated NiH electronic transitions the respective $\Delta J = \Delta\Omega$ branch shows a minimum overlap of ΔM subbranches with opposite polarization. There remains the question of whether this is a general rule for the Faraday geometry in magnetooptical spectroscopy since the overlap of ΔM subbranches depends on both the magnetic dipole moment and the rotational constant. Only for the case that both quantities are identical in the lower and upper electronic state the Q branch has no overlap of the different ΔM subbranches. And for identical rotational constant and doubling of the magnetic moment from lower to upper state, the R branch shows no overlap of the different ΔM subbranches. From this one would expect a different result for a molecular system with a large difference of the rotational constant of the lower and upper state. A more detailed investigation of this problem will be discussed in a forthcoming publication.

The alignment of pendular states is customarily characterized by the expectation value of $\cos\theta$. This quantity designates the average projection of the angular distribution of the molecular axis on the field direction. As the number of significant expansion terms in eq 2 grows, the $\langle\cos\theta\rangle$ increases with increasing field strength. Since the ICl(A−X) magnetic pendular transition line strengths are determined by only three terms of eq 3, the pendularization (which produces the alignment) at high field strengths causes a decrease of the respective line strength factor for P, Q, and R transitions. For the case of two paramagnetic levels more expansion coefficients are involved in the line strength factor (see refs 1 and 3). As the alignment of both states increases, the line strength factor increases, too. This very qualitative discussion of the alignment neglects the possible nonmonotonic variation of $\langle\cos\theta\rangle$ with field strength that appears at the transition from a Zeeman state into a bound pendular state for Zeeman eigenenergies larger than the free rotor eigenenergy. Its consequences for polarization spectroscopy on pendular states will be discussed in a forthcoming paper discussing polarization spectra between two pendular states of an electric dipolar molecule.

The agreement of calculated spectra with experiment was found for spectra taken over a range of the magnetic field strength from a few millitesla up to 500 mT. Further more detailed investigation of the line shape dependence on field strength, experimental resolution, and alignment parameter of the pendular states is in progress. The approximation for the calculation of polarization spectra that leads to eq 8 completely neglects the phase of the electromagnetic wave. Therefore, the simulated transmitted wave is necessarily linearly polarized. A preliminary experimental investigation shows evidence for a linear polarization of the transmitted wave. For each line of the polarization spectra it looks like there exists a detuning angle ζ for the second polarizer that tunes the detected signal down to zero. This would be impossible for elliptically polarized light. However, theoretical investigations of magnetooptical spectroscopy account for both dichroism (anisotropy of absorption) and birefringence (anisotropy of interference).[10] A more detailed study of this aspect is in progress.

5. Conclusion

The detection of the anisotropy of the figure axis of molecular pendular states was demonstrated experimentally using polarization spectroscopy. The high sensitivity of this experimental technique, which is directly related to magnetooptic spectroscopy, was demonstrated for the paramagnetic electronically excited A state of the ICl molecule. Except for the laser system, the apparatus used is a very simple, low-cost table-top setup. This was adequate to exhibit the capability of this technique to measure "low-temperature spectra" from room-temperature samples. The dramatic improvement offered is evident from comparisons with the simple absorption spectra of ICl and also with fluorescence excitation spectra of an ICl molecular beam.[19] Another advantage of polarization spectroscopy on pendular states is its ΔJ selectivity. A substantial reduction of lines in the spectra and characteristic line shapes both facilitate assignment of branches and determination of spectroscopic constants.

Theoretical considerations based on the idea of molecular pendular states led to a simple explanation of the spectral structures. Simple geometric arguments for the anisotropy in the absorption coefficient which causes the optical anisotropy of the paramagnetic sample in the magnetic field were used in connection with quantum mechanically calculated eigenstates and eigenenergies of pendular states to reproduce the measured spectra without any fitting parameter. This was found to be valid for magnetic field strengths up to 500 mT. The phase and therefore possible effects of birefringence are neglected in our model calculations. A theoretical approach for forward scattering magnetooptical spectroscopy shows that Faraday and Voigt effects are special solutions of a general equation.[10] This equation incorporates dispersion terms (responsible for birefringence) and absorption terms (responsible for dichroism). Both terms appear in the special solutions for Faraday and Voigt effects and are therefore also expected for our experiment. Besides the above-discussed experimental sources for peak level discrepancy between our measurements and our simulations, birefringence may be another source.

A polar molecule in an electric field[1,3,18] behaves much like a paramagnetic molecule in a homogeneous magnetic field. The method of producing anisotropy of transition moments in a molecular gas-phase sample should therefore easily be extendible to any molecule with a body-fixed electric dipole moment. Recently, this has been done in our laboratory.[19] The technique can even be extended to nonpolar, nonmagnetic molecules. Recently, Friedrich and Herschbach presented the theory of molecular pendular states created by a molecular dipole moment induced by a strong nonresonant laser field.[5] For this case only an anisotropy in the molecular polarizability is necessary; that occurs for any nonspherical molecule. The first experimental demonstration of laser-induced pendular states has been published very recently, observed in Raman spectra of naphthalene trimers.[6] Friedrich and Herschbach show that interaction parameters ω of the order of 100 are easily accessible with commercially available laser systems. Polarization spectroscopy on the other hand is very sensitive to the lowest rotational states of molecules already at interaction parameters that are only of the order of $\omega = 0.01$, as illustrated in Figure 5. Using laser systems of even moderate power focused to small spot sizes, optical anisotropy can be induced that should allow detection of spectra from samples at high temperature that reveal better selectivity and sparser spectral structures than spectra taken from samples at very low temperatures. In the same way this technique can be used either to determine electric or magnetic dipole moments of molecules, by means similar to fluorescence excitation spectra of pendular ICl,[20] or to make local measurements of electric or magnetic field strengths.

Acknowledgment. We have enjoyed support, encouragement, and helpful discussions with Professor Bernhard Dick and Professor Dudley R. Herschbach. We are also indebted to Dr. Jan Michael Rost for providing the computer code for the calculations of eigenenergies and line strength factors for pendular states.

References and Notes

(1) Friedrich, B.; Herschbach, D. R. *Nature* **1991,** *353*, 412. Friedrich, B.; Herschbach, D. R.; Rost, J.-M.; Rubahn, H.-G.; Renger, M.; Verbeek, M. *J. Chem. Soc., Faraday Trans.* **1993**, *89*, 1539.

(2) Slenczka, A.; Friedrich, B.; Herschbach, D. R. *Phys. Rev. Lett.* **1994,** *72*, 1806.

(3) Friedrich, B.; Slenczka, A.; Herschbach, D. R. *Can. J. Phys.* **1994,** *72*, 897.

(4) Loesch, H. J. *Annu. Rev. Phys. Chem.* **1995,** *46*, 555.

(5) Friedrich, B.; Herschbach, D. R. *Phys. Rev. Lett.* **1995**, *74*, 4623; *J. Phys. Chem.* **1995,** *99*, 15686.

(6) Kim, W; Felker, P. M. *J. Chem. Phys.* **1996**, *104*, 1147.

(7) Wieman, C.; Hänsch, T. W. *Phys. Rev. Lett.* **1976**, *36*, 1170. Song, J. J.; Lee, J. H.; Levenson, M. D. *Phys. Rev. A* **1978**, *17*, 1439.

(8) Dick, B. *Chem. Phys. Lett.* **1988,** *143*, 186; *Chem. Phys.* **1989**, *136*, 413; *Chem. Phys.* **1989**, *136*, 429.

(9) McCarthy, M. C.; Field, R. W. *J. Chem. Phys.* **1992**, *96*, 7237. McCarthy, M. C.; Bloch, J. C.; Field, R. W. *J. Chem. Phys.* **1994**, *100*, 6331. McCarthy, M. C.; Field, R. W. *J. Chem. Phys.* **1994**, *100*, 6347.

(10) Hirano, I.; *Phys. Rev. A* **1994**, *50*, 4650.

(11) Condon, E. U. *Phys. Rev.* **1928**, *31*, 891.

(12) von Meyenn, K. *Z. Phys.* **1970**, *231*, 154.

(13) Schlier, C. *Z. Phys.* **1955**, *141***,** 16.

(14) Choi, J. H.; Smith, D. W. *J. Chem. Phys.* **1965,** S189.

(15) Kryachko, E. S.; Yanovitskii, O. E. *Int. J. Quantum Chem.* **1991**, *40*, 33.

(16) Loison, J. C.; Durand, A.; Bazalgette, G.; White, R.; Audouard, E.; Vigue, J. *J. Phys. Chem.* **1995**, *99*, 13591.

(17) Herzberg, G. *Spectra of Diatomic Molecules*; Van Nostrand: New York, 1950.

(18) Durand, A.; Loison, J. C.; Vigue, J. *J. Chem. Phys.* **1994**, *101***,** 3514.

(19) Slenczka, A. To be published.

(20) Slenczka, A.; Friedrich, B.; Herschbach, R. D. *Chem. Phys. Lett.* **1994**, *224*, 238.

(21) Moore, C. A.; Davis, G. P.; Gottscho, R. A. *Phys. Rev. Lett.* **1984**, *52*, 538. Gottscho, R. A.; Mandich, M. L. *J. Vac. Sci. Technol. A* **1985**, *3*, 617. Mandich, M. L.; Gaebe, C. E.; Gottscho, R. A. *J. Chem. Phys.* **1985**, *83*, 3349. Gottscho, R. A. *Phys. Rev. A* **1987**, *36*, 2233.